CHEMICAL COMPOSITION, CRYSTALLINITY, AND THERMAL DEGRADATION OF BLEACHED AND UNBLEACHED KENAF BAST *(Hibiscus cannabinus)* PULP AND NANOFIBERS

Mehdi Jonoobi,[a,d] Jalaludin Harun,[a] Alireza Shakeri,[b] Manjusri Misra,[c] and Kristiina Oksman[d]*

Kenaf *(Hibiscus cannabinus)* nanofibers were isolated from unbleached and bleached pulp by a combination of chemical and mechanical treatments. The chemical methods were based on NaOH-AQ (anthraquinone) and three-stage bleaching (DEpD) processes, whereas the mechanical techniques involved refining, cryo-crushing, and high-pressure homogenization. The size and morphology of the obtained fibers were characterized by environmental scanning electron microscopy (ESEM) and transmission electron microscopy (TEM), and the studies showed that the isolated nanofibers from unbleached and bleached pulp had diameters between 10-90 nm, while their length was in the micrometer range. Fourier transform infrared (FTIR) spectroscopy demonstrated that the content of lignin and hemicellulose decreased in the pulping process and that lignin was almost completely removed during bleaching. Moreover, thermogravimetric analysis (TGA) indicated that both pulp types as well as the nanofibers displayed a superior thermal stability as compared to the raw kenaf. Finally, X-ray analyses showed that the chemo-mechanical treatments altered the crystallinity of the pulp and the nanofibers: the bleached pulp had a higher crystallinity than its unbleached counterpart, and the bleached nanofibers presented the highest crystallinity of all the investigated materials.

a: Institute of Tropical Forestry and Forest Products, University Putra Malaysia, Malaysia;
b: Department of Chemistry, Gorgan University, Iran; c: School of Engineering, Thornbrough Building, Guelph, Ontario, Canada d: Division of Manufacturing and Design of Wood and Bionanocomposites, Luleå University of Technology, Skellefteå, Sweden;
* Corresponding author: Kristiina Oksman, Department of Manufacturing and Design of Wood and Bionanocomposites, Luleå University of Technology, 931 87 Skellefteå, Sweden. Tel.: +46 910 58 53 71; fax: +46 910 58 53 99. E-mail address: kristiina.oksman@ltu.se (K. Oksman).

INTRODUCTION

In recent years, the use of lignocelluloses fibers as reinforcing agents for polymer matrices has advanced remarkably. These materials present numerous advantages, such as a low specific gravity, suitable mechanical properties, and recyclability. Furthermore, they can be obtained from renewable resources, have lower weights, and cost less than synthetic fibers of for instance carbon or glass (Li et al. 2000; Oksman 2000). The major components in lignocelluloses include cellulose, hemicellulose, and lignin. Cellulose is a linear polymer with both crystalline and amorphous regions, whereas lignin and

hemicellulose display a completely amorphous structure. Non-wood materials represent another type of cellulose source possessing a great potential for industrial applications (Mohanty et al. 2002). Kenaf is one of these non-wood lignocelluloses that grow in tropical and sub-tropical areas. Kenaf consists of two separate parts known as bast and core, of which the bast fibers have been found to possess attractive mechanical properties rendering them susceptible to be utilized as reinforcements in polymer composites as an alternative to glass fibers (Zampaloni et al. 2007; Ochi 2008; Xue et al. 2009; Sanadi et al. 1996; Liu et al. 2007). Recently, the Malaysian government has shown interest to support the development of new uses of kenaf crop (Mohd Edeerozey et al. 2007). Therefore the studies of kenaf fibers and separation to nanofibers are of interest.

Nano-sized reinforcements from renewable resources have gained an increased interest during the past years (Oksman and Sain 2006; Hubbe et al 2008). The expected advantages of nanofibers as compared to micro-sized fibers include an enhancement of the mechanical properties with a decrease in fiber size due to large surface areas (Oksman and Sain 2006). Cellulosic nanofillers from wood, wheat straw, soybean, hemp, etc., have already been employed as reinforcements in a variety of polymers to produce nanocomposites with improved mechanical properties (Chacraborty et al 2007; Wang and Sain 2007; Wang et al. 2007; Seydibeyoğlu and Oksman 2008; Alemdar and Sain 2008).

The cell wall of lignocellulosic fibers is comprised of basic structural units called microfibrils. These microfibrils are approx. 30-100 nm in diameter and a few micrometers in length (Wang et al. 2007). As a result, cellulose microfibrils can actually be considered to be nanofibers, since the definition of a nanofiber is a size <100 nm in one dimension (Gardner et al. 2008). These nanofibers include groups of cellulose chains that are bound together by hydrogen bonding. The hemicellulose and lignin form a matrix surrounding the cellulose microfibrils, which are the cementing materials in the plant cell wall. In order to efficiently isolate cellulose microfibrils (nanofibers), the removal of lignin and hemicellulose is essential.

Much attention has been paid to the study of nanofiber characteristics, which include decent mechanical properties, a high length-to-diameter ratio, an elevated crystallinity, etc. Numerous investigations have also concerned different isolation processes and the use of nanofibers as reinforcement in various polymer matrices. The studied isolation processes have been based on combined chemical and mechanical separation technologies or on entirely mechanical separation processes (Herrick et al. 1983; Turbak et al. 1983; Seydibeyoglu and Oksman 2008; Dinand et al. 1999; Dufresne et al. 2000; Alemdar and Sain 2007; Taniguchi and Okamura 1998).

NaOH-AQ (anthraquinone) pulping reduces the rate of degradation and causes less damage to cellulose chains, a fact that has been attributed to the stabilization effect of AQ on the cellulose macromolecules. Moreover, AQ has been found to block the active groups of cellulose and decrease the rate of oxidation (Helmy and Abd El Motagali 1993). The following constitutes a first report of the isolation of cellulose nanofibers from kenaf NaOH-AQ pulp. The main goal of this work was to combine chemical and mechanical processes in order to isolate nanofibers from raw kenaf. Microscopic techniques (TEM and ESEM) were used to characterize the morphology and size of the treated fibers, and the chemical composition of the fibers was measured before and after chemical treatments according to TAPPI standards. In addition, thermogravimetric

analysis (TGA), Fourier transform infrared (FTIR) spectroscopy, and X-ray analyses were employed to determine the properties of the isolated nanofibers.

EXPERIMENTAL

Materials

Raw kenaf bast *(Hibiscus cannabinus)* fibers were provided by an internal source in Malaysia, i.e., the Institute of Tropical Forestry and Forest Products (INTROP).

Methods

Pulping procedure

Kenaf bast fibers were cut to lengths of 2-3 cm. Subsequently, 300 g of oven–dried, short kenaf fibers were cooked in a digester (MK model, USA), with NaOH 15%, and 0.1% of anthraquinone (AQ). The ratio of cooking liquid to kenaf fibers was 7:1. The maximum cooking temperature was set to 160 $^{\circ}$C, and this temperature was reached after 60 min. Another 45 min of cooking were carried out at the maximum temperature. Table 1 lists the conditions of the NaOH-AQ pulping process.

Table 1. Conditions of NaOH-AQ Pulping Process

Cooking process	NaOH-AQ
NaOH	15%
AQ (anthraquinone)	0.1%
Liquor-to-fiber ratio	7:1
Maximum temperature	160 °C
Time to maximum temperature	60 min
Time at maximum temperature	45 min

Bleaching

In order to remove the residual lignin, a three-stage bleaching was performed. Table 2 shows the conditions of the bleaching processes.

Table 2. Conditions of the Bleaching Process

Stage	D1	Ep	D2
Chemical charge	Sodium chlorite (2%) Acetic acid (3%)	NaOH (1.5%) H_2O_2 (1%)	Sodium chlorite (1.25%) Acetic acid (3%)
Pulp consistency	10%	10 %	10%
Temperature	70 °C	70 °C	70 °C
Time	180 min	90 min	90 min

Mechanical Treatments

Bleached and unbleached kenaf pulps (with dry weights of 24 g) were immersed in distilled water for 8 hours. The fibers were distributed in the water using a laboratory disintegrator (Ihon-Rigoku-SP ¼ Japan model) at 3000 rpm for 20 min. A pulp mat, which has a total weight of 240 g, was prepared with 10% fiber concentration. With the purpose of defibrillating the fibers, the mat was then placed in a laboratory-type PFI mill (PTI Australian model) with a treatment level of 100,000 revolutions. Subsequently, the

refined pulp was immersed in liquid nitrogen, where it was subjected to a cryo-crushing process, as developed by Bhatnagar and Sain (2003). According to this method, the pulp was placed in liquid nitrogen and crushed using a mortar and pestle. Crushed pulp was then washed with distilled water and filtered.

Diluted suspensions (0.2 %) of bleached and unbleached pulp were prepared, and the nanofibers were individualized with a high pressure homogenizer (APV-1000). Prior to the homogenization process, all suspensions were ground in a mechanical blender apparatus for 15 min. The suspensions were passed through the homogenizer 40 times, and the pressure was held constant at 500 bar.

Characterization

Environmental scanning electron microscope (ESEM)

A Philips XL30 ESEM was used to study the effect of the treatments on the fiber morphology. The acceleration voltage was set to 20 kV, and all samples had been sputter-coated with gold to avoid charging. The fiber diameters were measured manually using an image analyzer program, XL Docu. Totally, 150 fibers from each material were measured, and the result was reported as a mean value of the data from each set of measurements.

Transmission electron microscope (TEM)

The structure and size of the nanofibers was studied by transmission electron microscopy on a Hitachi model H-7100. A drop of a diluted kenaf nanofiber suspension was deposited on a carbon-coated grid and allowed to dry at room temperature. Measurements of the fiber diameters after each treatment were carried out manually, using an image analyzer program, XL Docu. Totally, 150 fibers of each material were measured, and the result was reported as a mean value of the data from each set of measurements.

Chemical analysis

The chemical compositions of the kenaf fibers before and after chemical treatment were investigated. Soxhlet extraction with alcohol-acetone was carried out for 8 hours to calculate the content of the extract. The cellulose content extracted from the fibers was determined according to the TAPPI standard 203 om 93. Meanwhile, the percentage of holocellulose (Wise and Murphy 1946) and lignin, were determined according to TAPPI standards 222 om 88, as measured regularly after the chemical treatment. Each measurement was conducted in triplicate, and the obtained data were found to be highly reproducible.

Fourier transform infrared (FTIR) spectroscopy

Fourier transform infrared (FTIR) spectroscopy studies were performed on a Perkin-Elmer spectrometer 100 (USA) in order to determine changes in functional groups that may have been caused by the treatments. Prior to the analysis, 100 µm of the fibers were ground and mixed with KBr. The resultant suspensions were pressed into transparent pellets and analyzed in transmittance mode within the range of 4000-500 cm^{-1}.

X-ray diffraction

Structural and phase analyses of the samples were performed using an X-ray diffractometer (Philips P W 3040/60 X' pert Pro) with CuKα radiation (wavelength of 1.5405 Å) in step-scan mode (2θ range: 5-50˚). The phase identification of the samples was conducted using the X' Pert Highscore software with the support of the ICDD-PDF-2 database, and the lattice parameter was calculated using X'pert plus. The crystalline index of cellulose, C_{Ir}, was determined based on the empirical method (Segal et al 1959),

$$C_{Ir(\%)}= (I_{200}- I_{am})/ I_{200} \text{ x } 100 \tag{1}$$

where I_{200} is the peak intensity corresponding to cellulose I, and I_{am} is the peak intensity of the amorphous fraction.

Thermogravimetric analysis (TGA)

Thermogravimetric analysis was carried out to determine the thermal decomposition of the kenaf fibers after each treatment. The thermal stability data were obtained on a TGA/SDTA 851 (Mettler Toledo) thermogravimetric analyzer under linear temperature conditions. The temperature was swept from 25 ˚C to 550 ˚C at a heating rate of 10 ˚C/min under a nitrogen atmosphere.

RESULTS AND DISCUSSION

Chemical Composition

The chemical compositions of the kenaf fibers after various stages of chemo-mechanical treatments are presented in Table 3.

Table 3. Chemical Composition of Kenaf Fibers after Each Stage of Treatment

Materials	Cellulose (%)	Hemicelluloses (%)	Lignin (%)	Extractives (%)	Ash (%)
Raw kenaf	63.5 ± 0.5	17.6 ±1.4	12.7 ± 1.5	4.0 ±1.0	2.2 ± 0.8
Unbleached pulp	81.5 ±1.0	12.7 ±1.9	2.5 ± 0.3	0.9 ± 0.4	--
Bleached pulp	92.0 ±1.4	5.2 ± 0.6	0.5 ± 0.4	0.5 ± 0.3	--
Unbleached nanofiber	82.6 ± 0.9	11.8 ± 0.4	1.8 ± 0.4	0.8 ± 0.2	--
Bleached nanofiber	92.8 ± 0.5	4.7 ± 0.7	0.5 ± 0.3	0.4 ± 0.1	--

NaOH was found to be efficient in removing the lignin from the kenaf fibers: the lignin content decreased from 12.7 to 2.5 wt % in unbleached pulp fiber while the amount of hemicellulose was reduced from 17.6 to 12.7 wt%.

The three-stage bleaching process was used to increase the cellulose content in the pulp. Based on the chemical composition analysis, a majority of the lignin was removed from the bleached pulp, and the content of hemicellulose was found to be remarkably reduced. The final pulp presented a lignin content of 0.5% and a hemicellulose content of 5.2%.

In the first stage (D_1), sodium chlorite (Na_2ClO_2) and acetic acid gave rise to a high exodus of lignin and hemicellulose. In the second stage (Ep), hydrogen peroxide (H_2O_2) removed the residual chlorite in the pulp, thus rendering the removal of lignin more efficient. The last stage (D_2), was performed to further remove the hemicellulose and lignin. The results gathered from the chemical analysis after each treatment showed that the cellulose content was increased from 63.5% to 81.5% for the unbleached pulp, and further increased to 92% for the bleached pulp.

Morphology of the Treated and Untreated Kenaf Fibers

Figure 1 presents ESEM micrographs of the raw and chemo-mechanically treated kenaf fibers. It is clear from Fig. 1a that the raw kenaf fiber bundles where composed of individual fibers linked together by lignin. The image analysis demonstrated that the diameter of the raw kenaf fibers ranged from 10-80 µm, and more than 61% of the fibers were found to have diameters between 20 and 40 µm. Figures 1b and 1c show the structure of the fibers after the pulping and bleaching processes, respectively. It can be seen that these processes separated the fiber bundles to individual fibers and caused a significant decrease in their diameter. More than 79% of the unbleached pulp fibers had diameters between 5-15 µm, and more than 88% of the bleached pulp fibers displayed diameters between 1-8 µm. Figures 1d and 1e illustrate the morphology of the unbleached and bleached pulp fibers after the refining process and cryo-crushing, respectively. The image analysis study showed that 49% of the unbleached pulp fibers as well as 58% of the bleached pulp fibers now presented diameters within the range of 0.1-1 µm. These results proved that the PFI refining and cryo-crushing were capable of reducing the kenaf fiber diameter to the nanometer level. As can be seen from Figs. 1d and 1e, the fiber cell wall was broken and a larger surface area was created. It is also clear from the figures that the treatments were not strong enough to separate 100% of the nanofibers from the chemically treated kenaf pulp.
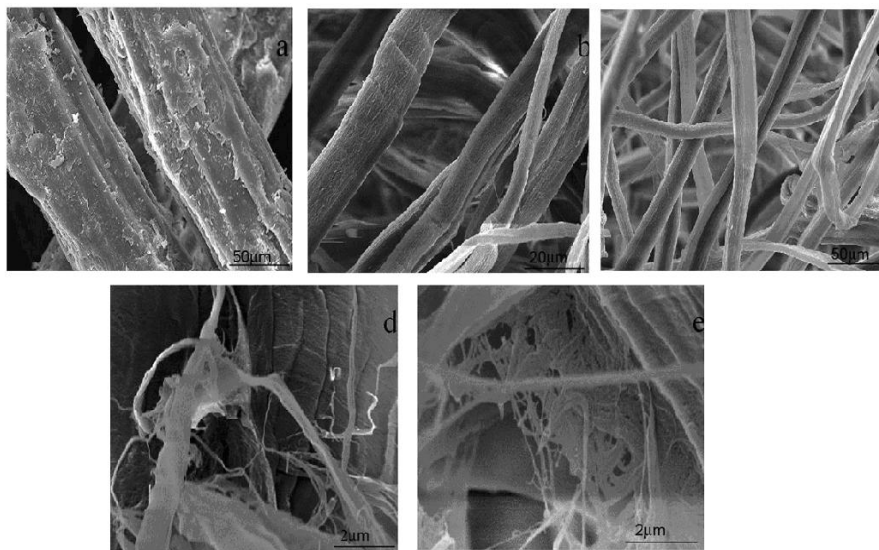

Fig. 1. ESEM micrographs of the structure of the kenaf fibers before and after chemical treatment for: a) raw kenaf fibers, b) unbleached pulp, c) bleached pulp, d) fibers after cryo-crushing and treatment in a PFI mill, and e) bleached pulp after cryo-crushing and treatment in a PFI mill

bioresources.com

A high-pressure homogenization was employed in the final step of isolating the refined and chemically treated kenaf pulp. Figure 2 shows TEM images of unbleached and bleached pulp after 40 passes through the high-pressure homogenizer, and these micrographs indicate that both pulp types were completely isolated to a nanosize level, i.e., below 100 nm. The fiber size distributions are presented in Fig. 3. It can be seen that the diameters of the homogenized unbleached and bleached nanofibers were very similar. More than 70% of the unbleached nanofibers had diameters in the range of 20-40 nm, with minimum and maximum values at 10 nm and 90 nm, respectively. Similarly, more than 70% of the bleached nanofibers displayed diameters between 10 and 30 nm. Here, the minimum value was 10 nm and the maximum was 70 nm. Moreover, the length of the obtained nanofibers was estimated to be several micrometers. The isolated nanofibers in this study were finer if compared to isolated fibers from wood and hemp (Seydibeyoğlu and Oksman 2008; Wang et al. 2007).
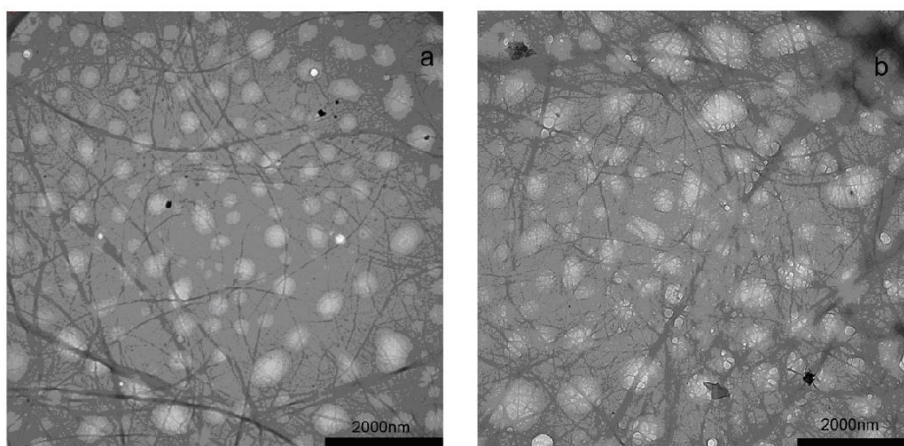

Fig. 2. Transmission electron micrographs of kenaf nanofibers after 40 pass through the high-pressure homogenizer: a) Unbleached nanofiber; b) bleached nanofiber (scale bar: 2000 nm).
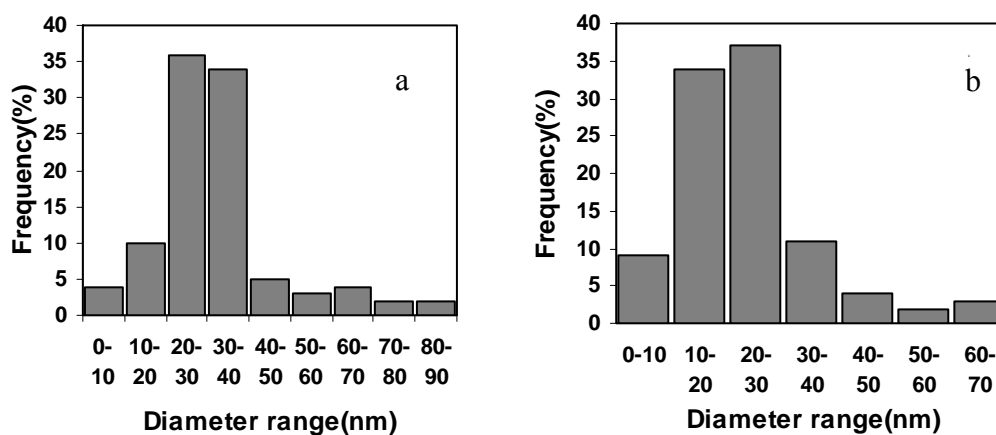

Fig. 3. Size distributions for the diameters of a) the homogenized unbleached pulp, and b) the homogenized bleached pulp

FTIR Analysis

FTIR spectroscopy was used to demonstrate the physical structure and functional groups of the lignocellulosic materials. The IR spectra of the untreated and treated fibers are shown in Fig. 4.
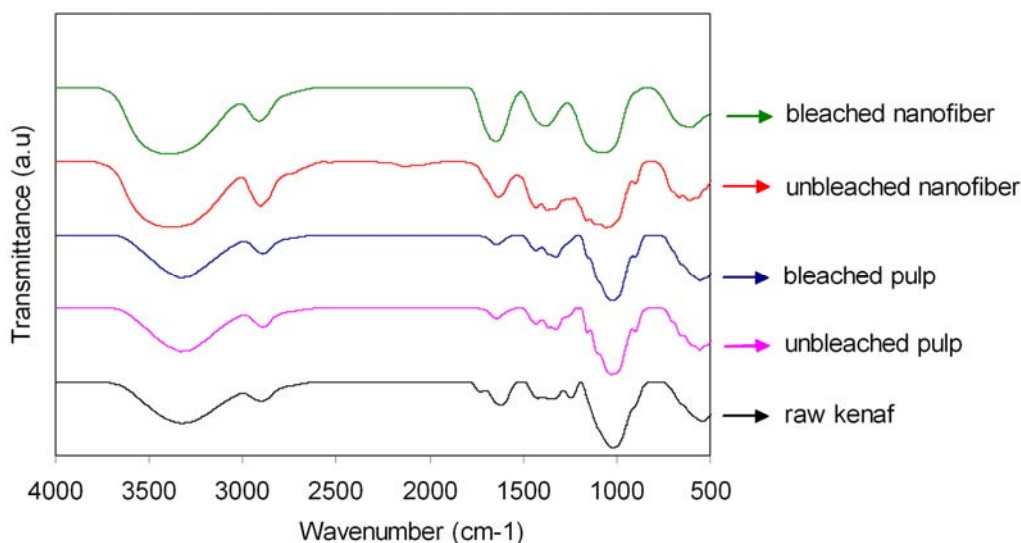

Fig. 4. Infrared spectra of the raw kenaf, unbleached pulp, bleached pulp, unbleached nanofibers and bleached nanofibers

The absorbance peaks in the 3400-3300 cm^{-1} region were attributed to the stretching of O-H groups, whereas those around 2900-2800 cm^{-1} were due to the stretching of C-H (Khalil et al. 2001). The peak located at 1731 cm^{-1} in the raw kenaf was assigned to the C=O stretching of the acetyl group in hemicellulose (Sgriccia et al. 2008; Tserki et al. 2005) or the ester linkage of carboxylic group in the ferulic and p-coumeric acids of lignin and/or hemicellulose (Alemdar and Sain 2007). This peak disappeared completely in the spectra of the unbleached and bleached pulps as well as for the bleached and unbleached nanofibers, thus indicating the removal of lignin and most of the hemicellulose during the chemical treatments.

In the raw kenaf, the peak at 1242 cm^{-1} was associated to the C-O stretching of the aryl group in lignin (Troedec et al 2008). The disappearance of this peak in the unbleached pulp, bleached pulp, unbleached nanofibers, and bleached nanofibers was believed to be due to the removal of lignin after the chemical treatments.

The absorbance between 1430-1431 cm^{-1} in the unbleached and bleached pulps was associated to the CH_2 symmetric bending (Troedec et al. 2008). The stretching of C-O and O-H can be observed as peaks around 1010-1070 cm^{-1} in all samples (Nacos et al. (2006).

The peaks observed in the range 1380-1320 cm^{-1} in all samples were attributed to the bending vibration of C-H and C-O groups of the aromatic ring in polysaccharides (Troedec et al. 2008; Nacos et al. 2006). The peaks in the region between 1650 and 1620 cm^{-1} for the raw kenaf, unbleached pulp, bleached pulp, as well as bleached and

bioresources.com

unbleached nanofibers were characterized by the adsorbed water (Troedec et al. 2008; Nacos et al. 2006). Meanwhile, the peaks at wave numbers 1382 cm^{-1} and 1371 cm^{-1} in the bleached and unbleached pulp nanofibers, respectively, reflected the C-H bending in polysaccharides (Troedec et al. 2008; Nacos et al. 2006). The absorbance peak at 1160 cm^{-1} in the kenaf pulp and unbleached nanofibers was due to the anti-symmetrical deformation of the C-O-C band (Silva et al 2008).

Finally, the vibration peak at 899 cm^{-1} in the unbleached pulp and unbleached nanofibers was assigned to the glycoside bonds, which are symmetric in polysaccharides (Troedec et al 2008). However, this peak was not found to be present in the bleached pulp and bleached nanofibers.

X-ray Diffraction

X-ray diffraction patterns are commonly used to calculate the crystallinity index, C_{Ir}. This was computed according to Segal's empirical method; cf. Eq (1) in the experimental section. Figure 5 presents X-ray diffractograms obtained for the five materials, and all samples presented major intensity peaks at a 2θ value close to 22.6° related to their crystalline structure.
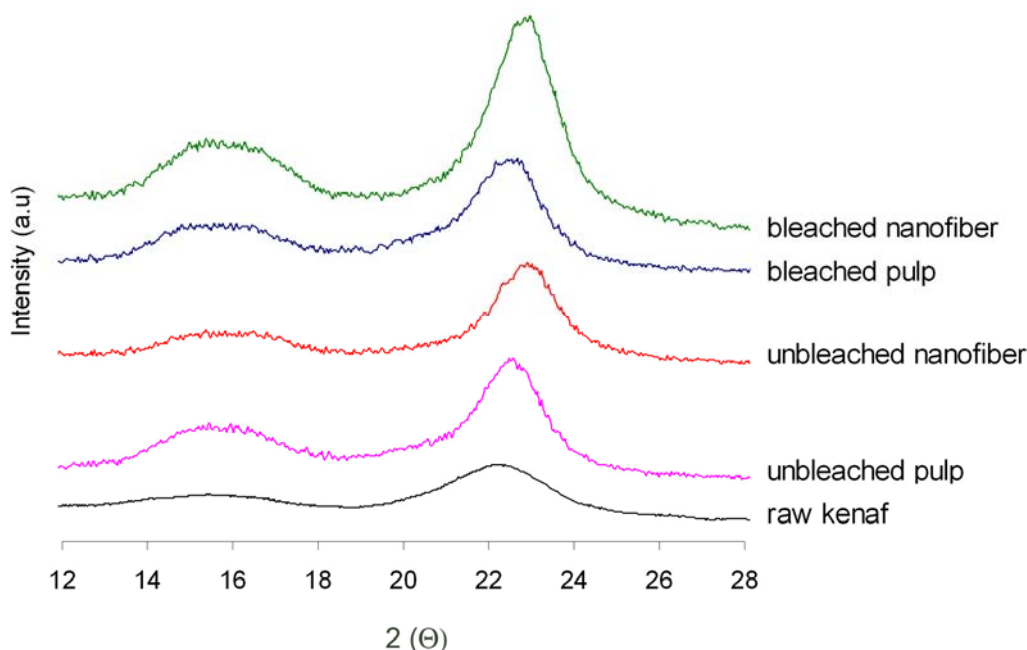

Fig. 5. X-ray diffraction patterns of the raw kenaf, unbleached pulp, bleached pulp, unbleached nanofibers, and bleached nanofibers.

The crystallinity index for the raw kenaf, the unbleached pulp, the bleached pulp, the unbleached nanofibers and the bleached nanofibers was found to be 48.2%, 68.1%, 77.3%, 79.2%, and 81.4%, respectively. These results clearly demonstrate the increase in the degree of crystallinity after chemo-mechanical treatments. The results also pointed towards the large difference in crystallinity between the raw kenaf fiber (48.2%) and the bleached nanofiber (81.4%). According to Alemdar and Sain (2007), such an increase in

the crystallinity index was expected after chemical treatment. Nonetheless, it might also be the result of the removal of lignin and hemicellulose, because of their amorphous nature. The results gathered from the X-ray diffraction measurements also demonstrated that the mechanical treatments could be affected by the degree of crystallinity in the cellulose fiber. Indeed, the proportion of crystalline regions was found to increase after subjection to the high-pressure homogenization. This was probably due to the nanofiber structure. On the other hand, cellulose nanofibers comprise pure cellulose chains, causing the crystallinity index to be higher. It is believed that the higher crystallinity leads to higher tensile strength of the fiber and thereby improved mechanical properties of the corresponding nanocomposites (Alemdar and Sain 2007).

Thermal Analysis

Thermogravimetric analysis (TGA) was carried out to investigate the suitability of the untreated and treated kenaf fibers for biocomposite processing. The underlying rationale was that many types of thermoplastic polymers require temperatures greater than 200°C in order to be processed. It is widely accepted that the primary thermal decomposition of cellulosic materials occurs between 200 and 400°C (Fisher et al. 2002). The initial decomposition of the cellulosic components takes place mostly in the amorphous regions (Mostashari and Fallah Moafi 2007). Figure 6 presents the thermogravimetric data corresponding to the kenaf fibers.
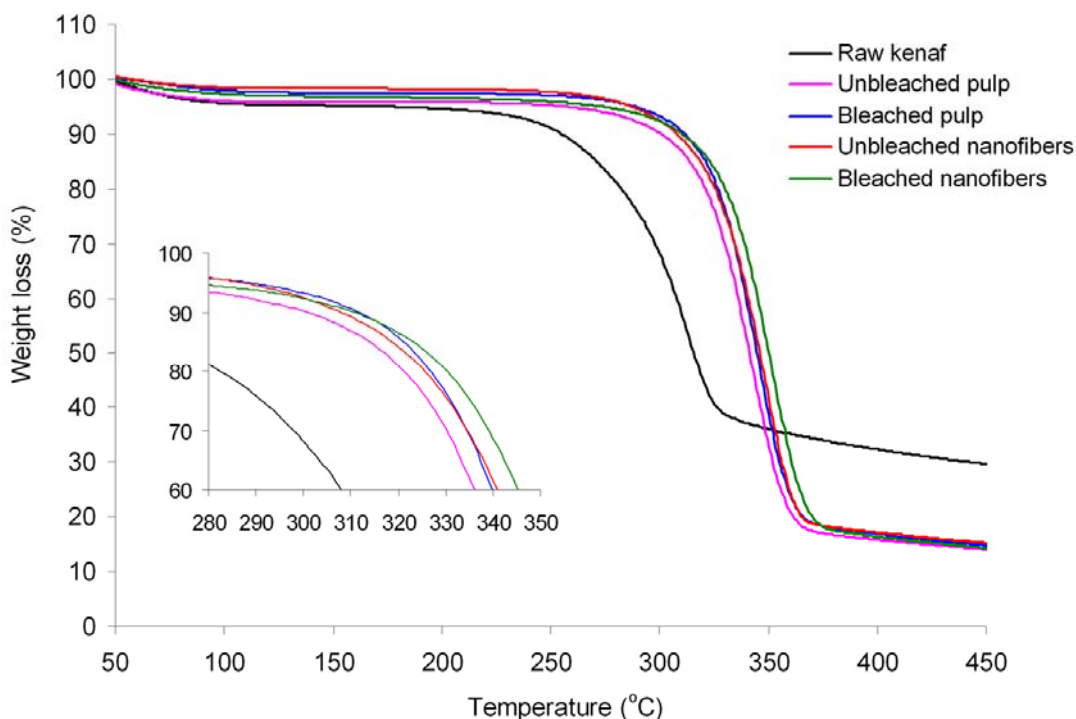

Fig. 6. TGA curves of raw kenaf, unbleached pulp, bleached pulp, unbleached nanofibers, and bleached nanofibers. The analysis was performed under a nitrogen atmosphere.

The TGA data in Fig. 6 illustrates an increasing thermal stability for the unbleached pulp, bleached pulp, as well as unbleached and bleached nanofibers, as compared to raw kenaf. The main degradation step (T_{max}) was found to be 313, 321, 342, 348, and 351°C for the raw kenaf, unbleached pulp, bleached pulp, unbleached nanofibers, and bleached nanofibers, respectively.

For the raw kenaf, the peak of T_{max} was attributed to the thermal degradation of hemicellulose (Yang et al. 2007), while the corresponding peak for the other samples indicated the decomposition of cellulose. Based on these results, the thermal stability of lignocellulosic materials was increased by the chemo-mechanical treatments. This could be attributed to the removal of hemicellulose and lignin during the chemical treatments, as well as to the higher degree of crystallinity in the material after mechanical processing. The alkaline and bleaching treatments were believed to degrade the amorphous region in the cellulose and increase the degree of crystallinity (Troedec et al. 2008; Ouajai and Shanks 2005). Consequently, the greater crystalline structure led to a high resistance towards heat and an increase in the maximum temperature for thermal degradation. The higher amount of residue in the raw kenaf fiber as opposed to in the fibers after chemo-mechanical treatments was due to the presence of ash as well as lignin, which have a very slow degradation (Ashori et al. 2006; Yang et al. 2007).

CONCLUSIONS

1. A chemical pulp from kenaf bast fibers was prepared based on a NaOH-AQ process. A three-stage bleaching procedure was carried out, including a DEpD stage for increasing the cellulose content in the produced pulp. Cellulose nanofibers were isolated using refining and homogenizing processes.
2. Microscopy studies revealed that the nanofiber diameters from the unbleached and bleached pulps were similar, between 10 and 90 nm. Moreover, their lengths were estimated to be at the micrometer scale.
3. The analysis of the chemical composition indicated an increase in the cellulose content after each chemical treatment; it thus changed from 63.5% in the raw kenaf fiber to 81.5% in the unbleached pulp and to 92% in the bleached pulp.
4. FTIR results also showed that the chemical treatments could successfully be used to remove lignin and hemicellulose.
5. Thermogravimetric analysis (TGA) revealed that the thermal stability increased in the materials having undergone chemo-mechanical treatments. This was believed to be due to the removal of hemicellulose and lignin as well as to an increase in crystallinity during processing.
6. X-ray analyses pointed at a higher crystallinity for the chemically treated fibers, and the highest crystallinity was found for the bleached nanofiber. Overall, the crystallinity increased from 48.2% in raw kenaf to 81.4% in the bleached nanofiber.

bioresources.com

ACKNOWLEDGMENTS

REFERENCES

Alemdar, A., and Sain, M. (2007). "Isolation and characterization of nanofibers from agricultural residues – Wheat straw and soy hulls," *Bioresour. Technol.* 99(6), 1664-1671.

Alemdar, A., and Sain, M. (2008). "Biocomposites from wheat straw nanofibers: Morphology, thermal and mechanical properties," *Compos. Sci. Technol.* 68(2), 557-565

Ashori, A., Jalaluddin, H., Raverty, W. D., and Mohd Nor, M. Y. (2006). "Chemical and morphological characteristics of Malaysia cultivated kenaf (*Hibiscus cannabinus*) fiber," *Polym-Plast Technol. Eng. J.* 45(1), 131-134.

Bodirlau, R., Teaca, C. A., and Spiridon, I. (2008). "Chemical modification of beech wood: Effect on thermal stability," *Bioresources* 3(3), 789-800.

Chakraborty, A., Sain, M., and Kortschot, M. (2005). "Cellulose microfibrils: A novel method of preparation using high shear refining and cryocrushing," *Holzforschung* 59(1), 102-107.

Dinand, E., Chanzy, H., and Vignon, M. R. (1999). "Suspensions of cellulose microfibrils from sugar beet pulp," *Food Hydrocolloids* 13, 275-283.

Dufresne, A., Dupeyre, D., and Vignon, M. R. (2000). "Cellulose microfibrils of starch-cellulose," *J. Appl. Polym Sci.* 76(14), 2080-2092.

Fisher, T., Hajaligol, M., Waymack, B., and Kellogg, D. (2002). "Pyrolysis behaviour and kinetics of biomass derived materials," *J. Anal. Appl. Pyrol.* 2(2), 331-349.

Gacitua, W. E., Ballerini, A., and Zhang, J. (2005). "Polymer nanocomposites synthetic and natural fillers. A review," *Ciencia y tecnología* 7(3), 159-178.

Gardner, D. J., Oporto, G. S., Mills, R., and Samir, M. A. (2008). "Adhesion and surface issues in cellulose and nanocellulose," *J. Adhesion Sci. Technol.* 22, 545-567.

Hajaligol, M., Waymack, B., and Kellogg, D. (2001). "Low temperature formation of aromatic hydrocarbon from pyrolysis of cellulosic materials," *Fuel* 80, 1799-1807.

Herrick, F. W., Casebier, R. L., Hamilton, J. K., and Sandberg, K. R. (1983). "Micro-fibrillated cellulose: Morphology and accessibility," *J. Appl. Polym Sci.* 37, 797-813.

Hubbe, M. A., Rojas, O. J., Lucia, L. A., and Sain, M. (2008). "Cellulosic nanocomposites: A review," *Bioresources* 3(3), 929-980.

Kamel, S. (2007) "Nanotechnology and its applications in lignocellulosic composites, A mini review," *eXPRESS Polym. Lett.* 1(9), 546-575.

Keshk, S., Suwinarti, W., and Sameshima, K. (2006). "Physicochemical characterization of different treatment sequences on kenaf bast fibers," *Carbohyd. Polym.* 65(2), 202-206.

Khalil, H. P. A., Ismail, H., Rozman, H. D., and Ahmad, M. N. (2001). "The effect of acetylation on interfacial shear strength between plant fiber and various matrices," *Eur. Polym. J.* 37(5), 1037-1045.

Khristova, P., Kordsachia, O., Patt, R., Khider, T., and Karrar, I. (2002). "Alkaline pulping with additives of kenaf from Sudan," *Ind. Crop Prod.* 15(3), 229-235.

Li, W., Wing, Y. M., and Ye, L. (2000). "Sisal fibre and its composites: A review of recent developments," *Compos. Sci. Technol.* 60(11), 2037-2055.

Liu, W., Drzal, L. T., Mohanty, A. K., and Misra, M. (2007). "Influence of processing methods and fiber length on physical properties of kenaf fiber reinforced soy based biocomposites," *Compos. Part B* 38(3), 352-359.

Mohanty, A. K., Misra, M., and Drzal, L. T. (2002). "Sustainable bio-composites from renewable resources: Opportunities and challenges in the green materials world," *J. Polym. Environ.* 10(1-2), 19-26.

Mohd Edeerozey, A. M., Akil, H. Md., Azhar, A. B., and Zainal Ariffin, M. I. (2007). "Chemical modification of kenaf fibers," *Mater. Lett.* 61, 2023–2025.

Mostashari, S. M., and Fallah, M. H. (2007). "Thermogravimetric analysis of a cellulosic fabric incorporated with ammonium iron (ii)-sulfate hexahydrate as a flame-retardant," *J. Indust. Textile.* 37(1), 31-42.

Nacos, M., Katapodis, P., Pappas, C., Daferera, D., Tarantilis, P. A., Christakopoulos, P., and Polissiou, M. (2006). "Kenaf xylan-A source of biologically active acidic oligosaccharides," *Carbohyd. Polym.* 66(1), 126-134.

Nakagaito, A. N., and Yano, H. (2005). "Novel high-strength biocomposites based on microfibrillated cellulose having nano-order-unit web-like network structure," *Appl. Phys. A.* 80(1), 155-159.

Nishimura, N., Izumi, A., and Kuroda, K. (2002). "Structural characterization of kenaf lignin: Differences among kenaf varieties," *Ind, Crop. Prod.* 15(2), 115-122.

Ochi, S. (2008). "Mechanical properties of kenaf fibers and kenaf/PLA composites," *Mechanics Mater.* 40(4-5), 446-452.

Oksman, K. (2000). "Mechanical properties of natural fiber mat reinforced thermo-plastic," *Appl. Compos. Mater.* 7(5-6), 403-414.

Oksman, K., and Sain, M., (2006). "Introduction to cellulose nanocomposites," *Cellulose Nanocomposites; Processing, Characterization and Properties,* ASC Symposium Series 938, Oxford Press, 2-8.

Ouajai, S., and Shanks, R. A. (2005). "Composition, structure and thermal degradation of hemp cellulose after chemical treatments," *Polym. Degrad Stab.* 89(2), 327-335.

Panthapulakkal, S., Zereshkian, A., and Sain, M. (2006). "Preparation and characterization of wheat straw fibers for reinforcing application in injection molded thermoplastic composites," *Bioresour. Technol.* 97(2), 265-272.

Sanadi, A. R., Roger, R. M., and Caulfield, D. (1996). "Agro-based fiber/polymer composites, blends and alloys," *Polym. News* 20, 7-17.

Seca, A., Cavaleiro, J., Domingues, F., Silvestre, A., Evtuguin, D., and Pascoal-Neto, C. (1998). "Structural characterization of the bark and core lignins from kenaf (*Hibiscus cannabinus*)," *J. Agric. Food Chem*. 46(8), 3100-3108.

Segal, L., Creely, L., Martin, A. E., and Conrad, C. M. (1959). "An empirical method for estimating the degree of crystallinity of native cellulose using X-ray diffractometer," *Textile. Res. J*. 29, 786-794.

Seydibeyoğlu, M. Ö., and Oksman, K. (2008). "Novel nanocomposites based on polyurethane and micro fibrillated cellulose," *Compos. Sci. Technol.* 68(3-4), 908-914.

Sgriccia, N., Hawley, M., and Misra, M. (2008). "Characterization of natural fiber surfaces and natural fibre composites," *Compos. Part A* 39(10), 1632-1637.

Silva, M. C., Lopes, O. R., Colodette, J. L., Porto, A. O., Rieumont, J., Chaussy, D., Belgacem, M. N., and Silva, G. G. (2008). "Characterization of three non-product materials from a bleached eucalyptus kraft pulp mill, in view of valorizing them as a source of cellulose fibres," *Ind. Crop Prod.* 27(3), 288-295.

Taniguchi, T., and Okamura, K., (1998). "New films produced from mircofibrillated natural fibres," *Polym. Int.* 47(3), 291-294.

Troedec, M., Sedan, D., Peyratout, C., Bonnet, J., Smith, A., Guinebretiere, R., Gloaguen, V., and Krausz, P. (2008). "Influence of various chemical treatments on the composition and structure of hemp fibers," *Compos. Part A* 39(3), 514-522.

Tserki, V., Zafeiropoulos, N. E., Simon, F., and Panayiotou, C. (2005). "A study of the effect of acetylation and propionylation surface treatments on natural fibers," *Compos. Part A* 36(8), 1110-1118.

Turbak, A. F., Snyder, F. W., and Sandberg, K. R. (1983). "Microfibrilated cellulose, A new cellulose product: Properties, uses, and commercial potential," *J. Appl. Polym Sci*.37, 815-827.

Wang, B., Sain, M., and Oksman, K. (2007). "Study of structural morphology of hemp fiber from the micro to the nanoscale," *Appl. Compos Mater.* 14(2), 89-103.

Wang, B., and Sain, M. (2007). "Dispersion of soybean stock-based nanofiber in a plastic matrix," *Polym. Int.* 56(4), 538-546.

Wise, L. E., and Murphy, M. (1946). "A chlorite holocellulose, Its fractionation and bearing on summative wood analysis and studies on the hemicelluloses," *Paper Trade J*. 122(2), 35-43.

Yang, H., Yan, R., Chen, H., Lee, D., and Zheng, C. (2007). "Characteristics of hemicellulose, cellulose, and lignin pyrolysis," *Fuel* 86, 1781-1788.

Xue, Y., Du, Y., Elder, S., Wang, K., and Zhang, J. (2009). "Temperature and loading rate effects on tensile properties of kenaf bast fiber bundles and composites," *Compos*. *Part B* 40(3), 189-196

Zampaloni, M., Pourboghrat, F., Yankovich, S. A., Rodgers, B. N., Moore, J. M., Drzal, L. T., Mohanty, A. K., and Misra, M. (2007). "Kenaf natural fiber reinforced polypropylene composites: A discussion on manufacturing problems and solutions," *Compos. Part A* 38(6), 1569-1580.